

Implementing Over 100 Command Codes for a High-Speed Hybrid Brain-Computer Interface Using Concurrent P300 and SSVEP Features

Minpeng Xu, Member, IEEE, Jin Han , Student Member, IEEE, Yijun Wang , Member, IEEE, Tzyy-Ping Jung , Fellow, IEEE, and Dong Ming , Senior Member, IEEE

Abstract—Objective: Recently, electroencephalography (EEG)-based brain-computer interfaces (BCIs) have made tremendous progress in increasing communication speed. However, current BCI systems could only implement a small number of command codes, which hampers their applicability. **Methods:** This study developed a high-speed hybrid BCI system containing as many as 108 instructions, which were encoded by concurrent P300 and steady-state visual evoked potential (SSVEP) features and decoded by an ensemble task-related component analysis method. Notably, besides the frequency-phase-modulated SSVEP and time-modulated P300 features as contained in the traditional hybrid P300 and SSVEP features, this study found two new distinct EEG features for the concurrent P300 and SSVEP features, i.e., time-modulated SSVEP and frequency-phase-modulated P300. Ten subjects spelled in

both offline and online cued-guided spelling experiments. Other ten subjects took part in online copy-spelling experiments. **Results:** Offline analyses demonstrate that the concurrent P300 and SSVEP features can provide adequate classification information to correctly select the target from 108 characters in 1.7 seconds. Online cued-guided spelling and copy-spelling tests further show that the proposed BCI system can reach an average information transfer rate (ITR) of 172.46 ± 32.91 bits/min and 164.69 ± 33.32 bits/min respectively, with a peak value of 238.41 bits/min (The demo video of online copy-spelling can be found at <https://www.youtube.com/watch?v=EW2Q08oHSBo>). **Conclusion:** We expand a BCI instruction set to over 100 command codes with high-speed in an efficient manner, which significantly improves the degree of freedom of BCIs. **Significance:** This study holds promise for broadening the applications of BCI systems.

Manuscript received August 31, 2019; revised December 28, 2019; accepted February 12, 2020. Date of publication March 3, 2020; date of current version October 20, 2020. This work was supported in part by the National Key Research and Development Program of China under Grant 2017YFB1300302, in part by the National Natural Science Foundation of China under Grants 81630051, 81601565, and 61671424, in part by Tianjin Key Technology R&D Program under Grant 16ZXHLSY00270, in part by the Young Elite Scientist Sponsorship Program by CAST under Grants 2018QNRC001, and in part by the Strategic Priority Research Program of Chinese Academy of Science under Grant XDB32040200. (Minpeng Xu and Jin Han contributed equally to this work.) (Corresponding authors: Yijun Wang; Dong Ming.)

Minpeng Xu is with the Laboratory of Neural Engineering and Rehabilitation, Department of Biomedical Engineering, College of Precision Instruments and Optoelectronics Engineering, Tianjin University, and also with the Tianjin International Joint Research Center for Neural Engineering, Academy of Medical Engineering and Translational Medicine, Tianjin University.

Jin Han is with the Laboratory of Neural Engineering and Rehabilitation, Department of Biomedical Engineering, College of Precision Instruments and Optoelectronics Engineering, Tianjin University.

Yijun Wang is with the State Key Laboratory on Integrated Optoelectronics, Institute of Semiconductors, Chinese Academy of Sciences, Beijing 100083, China (e-mail: wangyj@semi.ac.cn).

Tzyy-Ping Jung is with the Swartz Center for Computational Neuroscience, University of California, and also with the Laboratory of Neural Engineering and Rehabilitation, Department of Biomedical Engineering, College of Precision Instruments and Optoelectronics Engineering, Tianjin University.

Dong Ming is with the Laboratory of Neural Engineering and Rehabilitation, Department of Biomedical Engineering, College of Precision Instruments and Optoelectronics Engineering, Tianjin University, Tianjin 300072, China, and also with the Tianjin International Joint Research Center for Neural Engineering, Academy of Medical Engineering and Translational Medicine, Tianjin University, Tianjin 300072, China (e-mail: richardming@tju.edu.cn).

Digital Object Identifier 10.1109/TBME.2020.2975614

Index Terms—P300, steady-state visual evoked potential (SSVEP), high-speed, hybrid BCI, concurrent EEG features, large instruction set.

I. INTRODUCTION

RAIN-COMPUTER interfaces (BCIs) provide a special pathway for the brain to directly communicate with the environment, which does not depend on the peripheral neuromuscular system [1], [2]. Recently, vision-based BCI systems, which have higher bit rates over other BCI systems, have made tremendous progress and gained increasing attention from researchers [3]–[8]. Specifically, P300-based speller [8]–[12], the steady-state visual evoked potential (SSVEP)-based BCI [13]–[15] and their hybrids [16]–[19] are the most popular paradigms. A new visual BCI paradigm has been recently developed to significantly reduce visual fatigue by sharply reducing the stimulus size [20].

The performance of a BCI is normally evaluated by the total number of commands, the time needed to output a command and command-selection accuracy. Information transfer rate (ITR) [1], [21] quantitatively formulates the relation between these three factors and system performance. Previous BCI studies mainly focused on how to increase accuracy and decrease the time needed to output a command to improve the system performance but show less interest in the expansion of the instruction set. Since the first P300-speller, which was developed in 1988 [22], there have always been only up to tens of instructions for

BCI systems. Specifically, Hwang introduced an SSVEP-based BCI keyboard with 30 LEDs flicking at different frequencies [23]. Chen *et al.* proposed a joint frequency-phase modulation method (JFPM) that encoded 40 instructions for SSVEP-BCI [21], [24]. Townsend *et al.* developed a P300-based BCI with 72 alphanumeric characters and keyboard commands [25]. Jin *et al.* designed an adaptive method for P300 speller to encode 84 instructions [26]. **It is worth noting that there exists a compromise between the number of instructions and the other two factors**, i.e., a larger number of instructions would often increase the time needed to output a command and reduce accuracy to complete a mental selection, which would in return hurt the ITR. Therefore, increasing the number of instructions might reduce the overall performance of the BCI system. **However, if this attempt proves successful, it will considerably improve the practicality of BCIs in real-world applications. To our best knowledge, no study has yet implemented over 100 commands for BCIs, which requires a delicate design to balance the aforementioned factors.**

The encoding strategy is an eternal topic of BCIs. From the view of telecommunication systems, the information stream of visual BCIs is analogous to the signal in multiple access channels [5]. Specifically, a P300 speller has the same idea of time division multiple access (TDMA), which assigns each character to an independent time interval. The SSVEP-based BCI uses the frequency division multiple access (FDMA), which tags each character with a specific flickering square whose frequency is different from each other. Theoretically, the P300 speller could encode an infinite number of instructions, but the overall performance will sharply degrade when the consuming time increases [27]. In contrast, the time used for encoding SSVEP-BCI instructions is very short, but the narrow EEG band limits the number of SSVEP frequencies [28], [29]. Therefore, a combination of the two BCI paradigms may overcome their shortcomings and expand the instruction set in an efficient manner. Previous studies on the hybrid P300-SSVEP BCIs have demonstrated the advantages of such combination [17]–[19], [30], [31].

This study aimed to explore a new hybrid P300-SSVEP BCI system that can effectively communicate a large number of instructions. By incorporating the steady-state visual stimulus (SSVS) into the P300 speller, we developed a 108-instruction BCI system containing twelve parallel 3×3 P300 sub-spellers. Notably, different from the traditional P300 paradigm, characters in each sub-speller were individually highlighted by a 200 ms-long SSVS rather than a transient visual stimulus. Therefore, the target stimulus could elicit both a larger P300 and a larger time-modulated SSVEP than the non-target stimulus. As the SSVS were different for each sub-speller, they would elicit different SSVEPs. According to our previous studies [30], [32], [33], the transient event-related potentials (ERP) would be modulated into different shapes by the different background SSVEPs, as phase resetting may explain the generation of ERP, which is a non-linear process. Thus, both P300 and SSVEP should contribute to the recognition of the target character and the sub-speller, resulting in efficient target identification. The time needed to output a command is 1 second in this design, which is sufficient for all participants to perform a correct

selection together with an additional cue time of 0.7 seconds. It's worth noting that the proposed hybrid system had two advantages. One advantage was that it successfully expanded the instruction set to 108 while ensuring the speed of BCI. The other advantage was that the SSVS duration of each character was only 200 ms in this study, which was considerably shorter than the previous lowest limit of 300 ms [34]. The decrease of the SSVS duration can effectively reduce the risk of visual fatigue.

II. MATERIALS AND METHODS

A. Subjects

Ten healthy volunteers (3 females and 7 males, 21–26 years of age, all right handed) with normal or corrected to normal vision participated in both offline and online cue-guided spelling experiments. Another group of ten subjects participated in an online copy-spelling experiment. Three of them (i.e., S3, S5, S9) also took part in the offline and online cued-guided spelling experiments (corresponding to S1, S2, S7, respectively). The Institutional Review Board at Tianjin University approved the experimental procedures. All subjects were fully informed of all procedures and signed an informed consent agreement, in accordance with the Declaration of Helsinki, and including a statement that they have known all possible consequences of the study.

B. A Hybrid P300-SSVEP BCI Speller Paradigm

The visual stimuli were presented on a 27-inch liquid-crystal display (LCD) monitor whose resolution was $1,920 \times 1,080$ pixels and refresh rate was 120 Hz. A 9×12 matrix showed 108 black characters on a white background (see Fig. 1(a)). They were further divided into 12 small 3×3 matrices. Each small matrix was an independent P300 sub-speller whose characters were individually highlighted by a gray square in a random and ergodic sequence. Each stimulation square subtended 1.49 degrees of visual angle in the vertical direction and 1.78 degrees in the horizontal direction. The stimulus duration for each character was 200 ms and the inter-stimulus interval (ISI) was -100 ms. It was worth noting that the duration of the inter-target stimulus was greater than 700 ms (the interval for cue presentation and gaze switching).

So there were no attentional blink and repetition blindness. All sub-spellers were triggered at the same time. Therefore, it needed only 1 second to run a complete cycle for 108 characters, which was defined as a 'round' in this study. Different from the traditional P300 paradigm, the stimulation square changed its grayscale in a sinusoidal mode whose frequency and initial phase were different for each sub-speller, as shown in Fig. 1(b), 1(c) and 1(d). This study used the sampled sinusoidal stimulation method [15] to present visual flickers using the refresh rate. The frequencies and phases of the 12 flickering stimuli were determined with the JFPM method [21]. To separate the SSVEP frequency band from the P300 frequency band, the 12 flickering frequencies were selected above 12 Hz, from 12.4 to 14.6 Hz with a step of 0.2 Hz. According to [35], SSVEPs with any

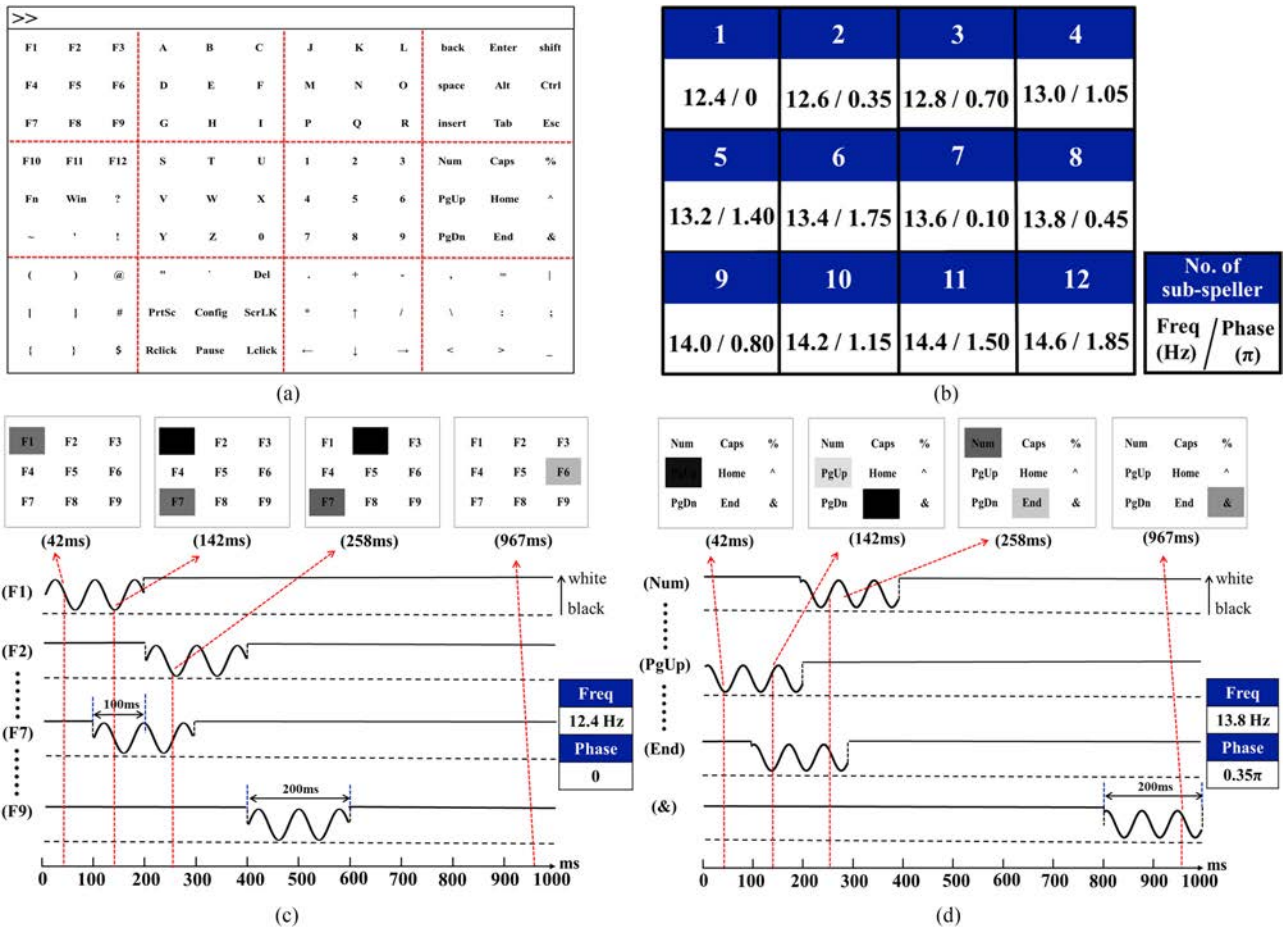


Fig. 1. Illustration of the stimulation in the hybrid BCI speller. (a) Distribution of 108 characters on the screen was divided into 12 sub-spellers by the red dash lines. The characters on the stimulus interface were distributed according to a certain rule. For example, alphanumeric keys were arranged in order and were placed at sub-speller 2, sub-speller 3, sub-speller 6, and sub-speller 7 (i.e., the center of the interface). (b) The selected frequency and initial phase of stimulation squares were displayed for each sub-speller. (c) Stimulation process for sub-speller 1. The red dotted lines with arrows indicate specific time points. (d) Stimulation process for sub-speller 8.

stimulation phase for 40 frequencies (ranging from 8 Hz to 15.8 Hz with step of 0.2 Hz), which covered all the stimulation frequencies of this experiment, can be simulated by a simulation method. Therefore, the initial phases were optimized by a search of phase interval (from 0 to 2π with a step of 0.05π) of the JFPM method on a public SSVEP dataset using the simulation method with a stimulus duration of 200 ms, resulting in a phase interval of 0.35π between two neighboring frequencies. For more details, please refer to [35]. The stimulation program was developed under MATLAB (MathWorks, Inc.) using the Psychophysics Toolbox Version3.

C. BCI Experiment

Participants sat in front of the monitor screen with a distance of 60 cm. They were asked to focus on the target character indicated beforehand and count the number of times the target was highlighted. In the offline experiment, the character specified for selection would be indicated by an underneath red triangle with 0.79 degrees of visual angle for 0.7 seconds. Then the visual

stimulus ran for five successive rounds for all the characters, which last 5 seconds, i.e., the subject chose the same target for five times. Each round contained 1 target stimulus and 8 non-target stimuli. All subjects were required to spell all 108 characters on the screen, which were divided into three blocks (36 characters in each block). They would have a break of several minutes between two successive blocks. The offline experiment lasted about 13 minutes for each subject.

In the online experiments, all subjects were asked to spell 24 specified characters (two characters in each of the twelve sub-spellers). There were two types of online tasks (i.e., cued-guided spelling and copy-spelling experiments). Classification algorithm and the other aspects of the two online experiments were completely consistent except for with or without visual cues. For online cued-guided spelling experiments, the subjects were the same as the offline experiments. The target character would be indicated by an underneath red triangle for 0.7 seconds within which the subjects need to shift their attention to the character and be prepared for the upcoming stimuli. Visual feedback (i.e., the target character determined by an online data analysis



Fig. 2. The total flow diagram of signal processing.

program) was presented to the text input field on the top of the speller (see Fig. 1(a)) in real time. The online copy-spelling experiments were implemented with another group of ten subjects. Before the experiment, the subjects were trained to remember the position of each character and they were told the characters they would spell in the experiment. Therefore, they were able to shift their fixation points very fast from character to character in 0.7 second without visual cues at the target characters. All target characters were presented in a line on top of the text input field during the copy-spelling task. Visual feedbacks of characters determined by the online data analysis program were typed below the line of target characters in real time. For each subject, the same offline data collection and analysis procedures were implemented before the online copy-spelling experiment. In both cued-guided and copy-spelling experiments, only one round was used for the online spelling test.

D. EEG Recording and Processing

EEG signals were recorded using a Neuroscan Synamps2 system with 13 electrodes placed at Fz, Cz, Pz, PO3, PO4, PO5, PO6, PO7, PO8, POz, O1, Oz and O2 according to the International 10/20 system. The reference electrode was placed on the left mastoid and the ground electrode was placed on the prefrontal lobe. The recorded signals were band-pass filtered at 0.1–200 Hz and notch filtered at 50Hz, digitized at a rate of 1,000 Hz and then stored in a computer.

In the recognition process, there were two sequential steps: (1) recognizing the sub-speller containing the target character and then (2) recognizing the target character within the identified sub-speller, as shown in Fig. 2. Fig. 3 shows the signal-processing flows and the corresponding methods used in this study. Here, we compared the classification results of single-modality EEG features (i.e., P300, SSVEP) and hybrid EEG features using different classification methods for both recognition steps. The parameters of time windows and filters were selected according to previous studies [21], [24] and further optimization towards the best classification performance in offline data analysis.

Fig. 3(a) shows the process of sub-speller recognition using SSVEP. The EEG signals of nine channels (Pz, PO5, PO3, POz, PO4, PO6, O1, O2, and Oz) [34] were filtered by a filter bank (containing seven Chebyshev Type I filters) into $[X \text{ Hz}, 92 \text{ Hz}]$ ($X = 11, 22, 34, 46, 58, 70 and 82), and then down-sampled to 250 Hz. For each sub-band, the SSVEP samples were extracted from 140 ms to 340ms. The extended canonical correlation analysis (CCA) [21] and ensemble task-related component analysis (TRCA) [34] were then used to recognize SSVEP. The outputs indicated the predicted sub-speller.$

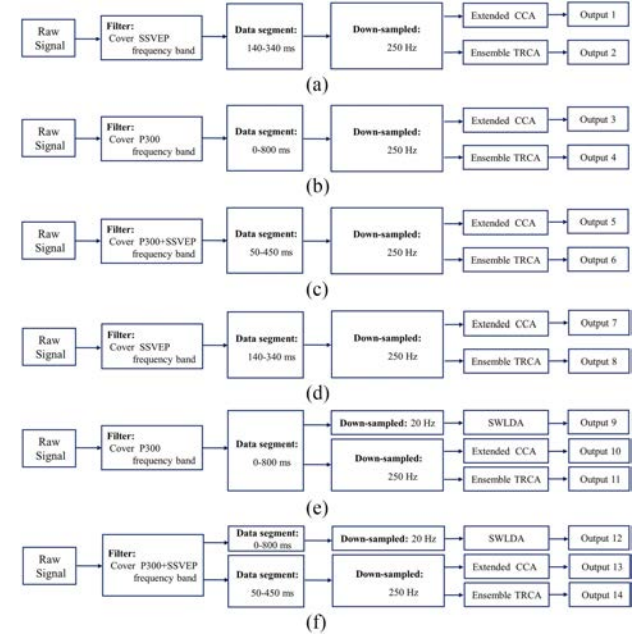


Fig. 3. The flow diagram of signal processing. The sub-speller was identified using (a) single SSVEP feature, (b) single P300 feature or (c) hybrid features. The target character within sub-speller was identified using (d) single SSVEP feature, (e) single P300 feature or (f) hybrid features.

Fig. 3(b) shows the process of sub-speller recognition using P300. It is typically measured most strongly by the electrodes covering the parietal lobe [18]. The EEG signals of six channels (Fz, Cz, Pz, PO7, PO8, and Oz) were filtered to 1–10 Hz with Chebyshev type I filters, and then down-sampled to 250 Hz. The P300 features extracted from 0 ms to 800 ms were classified by the extended CCA and ensemble TRCA, respectively. The outputs indicated the predicted sub-speller.

Fig. 3(c) shows the process of sub-speller recognition using hybrid features. The EEG signals of eight channels (Fz, Cz, Pz, PO7, PO8, O1, O2, and Oz) were filtered by a filter bank (including eight Chebyshev Type I filters) into $[X \text{ Hz}, 92 \text{ Hz}]$ ($X = 11, 22, 34, 46, 58, 70 and 82). As shown in Fig. 4, the hybrid features were significantly separable between 100 and 400 ms. And after experimenting with different time windows, we found that the time window of 50–450 ms achieved better results for the hybrid features. Extended CCA and TRCA were then used to recognize SSVEP, respectively. The outputs indicated the predicted sub-speller.$

Fig. 3(d) shows the process of character recognition within sub-speller using SSVEP. Parameters and settings were the same as Fig. 3(a). The outputs indicated the predicted character within the sub-speller.

Fig. 3(e) shows the process of character recognition within sub-speller using P300. The classic stepwise linear discriminant analysis (SWLDA) was used and compared with the extended CCA and the ensemble TRCA. The EEG signals of channel Fz, Cz, Pz, PO7, PO8, and Oz were filtered to 1–10 Hz with Chebyshev type I filters, and then down-sampled to 20 Hz for SWLDA

classification, and 250 Hz for extended CCA and TRCA. The P300 features used for classification were extracted from 0 ms to 800 ms. The outputs indicated the predicted character within the sub-speller.

Fig. 3(f) shows the process of character recognition within sub-speller using hybrid features. For the extended CCA and ensemble TRCA, the parameters were the same as Fig. 3(c). For the SWLDA, the data were filtered to 1–17 Hz and extracted from 0 ms to 800 ms.

E. Step-Wise Linear Discriminant Analysis

SWLDA works well in recognizing P300 potentials for the hybrid P300-SSVEP BCIs [37]. SWLDA is an extension of Fisher linear discriminant (FLD) analysis, which reduces feature space by selecting the most significant features for the discriminant function. A combination of forward and backward stepwise analyses was implemented in SWLDA. The input features are weighted using ordinary least-squares regression (equivalent to FLD) to predict target class labels. Starting with no initial features in the discriminant function, the most statistically significant input feature for predicting target label is added to the discriminant function. After each new entry to the discriminant function, a backward stepwise analysis is performed to remove the least significant input features. This procedure ensures that the regression equation only contains significant variables before each new variable is introduced. This process is repeated until the discriminant function includes a predetermined number of features or until no additional features satisfy entry/removal criteria. In this study, the p-value for entry was set to <0.1 , while for removal was set to >0.15 . The predetermined number of features was set to 60.

F. Extended Canonical Correlation Analysis

CCA is a statistical way to measure the linear relationship between two multidimensional variables, which may have some underlying correlation [38], [39]. Considering two multidimensional variables X , Y and their linear combinations $x = X^T W_X(X, Y)$ and $y = Y^T W_Y(X, Y)$, CCA finds the weight vectors, $W_X(X, Y)$ and $W_Y(X, Y)$, which maximize the correlation between x and y . For the extended CCA, there are three multi-dimensional variables: multi-channel EEG test data $X^{(m)} \in \mathbb{R}^{N_c \times N_s \times N_t}$, individual template obtained by averaging multiple training trials as $\bar{X}^{(m)} \in \mathbb{R}^{N_c \times N_s}$, and sine-cosine reference signals Y_f [21]. N_c is the number of channels, N_s is the number of sample points, and N_t is the number of trials. The correlation coefficient between the projections of two variables using the CCA-based method is used to identify the target. We define the following three weight vectors obtained by CCA: (1) as shown bottom of this page, $W_X^{(m)}(X^{(m)}, Y_f)$ between the test data $X^{(m)}$ and reference signals Y_f ; (2) $W_X^{(m)}(X^{(m)}, \bar{X}^{(m)})$ between the test data $X^{(m)}$ and individual template $\bar{X}^{(m)}$; (3) $W_{\bar{X}^{(m)}}(\bar{X}^{(m)}, Y_f)$ between individual template $\bar{X}^{(m)}$ and reference signals Y_f . Furthermore, in CCA between $X^{(m)}$ and $\bar{X}^{(m)}$, $W_X^{(m)}(X^{(m)}, \bar{X}^{(m)})$ and $W_{\bar{X}^{(m)}}(X^{(m)}, \bar{X}^{(m)})$ represent

the weight vector for $X^{(m)}$ and $\bar{X}^{(m)}$, respectively. The correlation coefficient is calculated as [21], [34]

$$\hat{r}_n^{(m)} = \begin{bmatrix} r_{n,1}^{(m)} \\ r_{n,2}^{(m)} \\ r_{n,3}^{(m)} \\ r_{n,4}^{(m)} \\ r_{n,5}^{(m)} \end{bmatrix} = \begin{bmatrix} \rho(X^{(m)T} W_X^{(m)}(X^{(m)}, Y_f), Y_f^T W_Y^{(m)}(X^{(m)}, Y_f)) \\ \rho(X^{(m)T} W_X^{(m)}(X^{(m)}, \bar{X}^{(m)}), \bar{X}^{(m)T} W_X^{(m)}(X^{(m)}, \bar{X}^{(m)})) \\ \rho(X^{(m)T} W_X^{(m)}(X^{(m)}, Y_f), \bar{X}^{(m)T} W_{\bar{X}^{(m)}}(X^{(m)}, Y_f)) \\ \rho(X^{(m)T} W_{\bar{X}^{(m)}}(\bar{X}^{(m)}, Y_f), \bar{X}^{(m)T} W_{\bar{X}^{(m)}}(\bar{X}^{(m)}, Y_f)) \\ \rho(\bar{X}^{(m)T} W_X^{(m)}(X^{(m)}, \bar{X}^{(m)}), \bar{X}^{(m)T} W_{\bar{X}^{(m)}}(X^{(m)}, \bar{X}^{(m)})) \end{bmatrix} \quad (1)$$

where m indicates the index of sub-bands designed by filter bank ($m \in [1, N_b]$), n indicates the index of sub-spellers ($n \in [1, 12]$) and $\rho(a, b)$ indicates the Pearson's correlation analysis between a and b . The five features and correlation coefficients in different sub-bands are weighted by the following equations [24]:

$$R_n^{(m)} = \sum_{l=1}^5 \text{sign}(r_{n,l}^{(m)}) * (r_{n,l}^{(m)})^2 \quad (2)$$

$$\rho_n = \sum_{m=1}^{N_b} (m^{-1.25} + 0.25) * (R_n^{(m)})^2 \quad (3)$$

where $\text{sign}()$ is symbolic function and N_b indicates the number of sub-bands (The value of N_b using different selected features was different. For P300, $N_b = 1$. For SSVEP, $N_b = 7$. For hybrid features, $N_b = 8$). In practice, target can be identified by the following equation:

$$\tau_t = \arg \max_n \rho_n \quad (4)$$

where n is the index of test data trials (The number of n was different in different conditions. For sub-speller recognition, n ranged from 1 to 12. For character recognition within the specified sub-speller, n ranged from 1 to 9). Target class τ_t can be identified by equation (4).

G. Ensemble Task-Related Component Analysis

The Ensemble TRCA has been proved the most powerful recognition algorithm for SSVEP classification [34], [40]. TRCA is an algorithm that finds projection matrix $W = [w_{j_1} w_{j_2} \dots w_{N_c}]^T$ to maximize the covariance of task-related components between trials [41]. j_1 and j_2 refer to the index of channels. Specifically, for the recorded N_c -channels EEG signal $x(t) \in \mathbb{R}^{N_c}$ (The value of N_c using different features varied. For P300, $N_c = 6$. For SSVEP, $N_c = 9$. For hybrid features, $N_c =$

8.), all possible combinations of trials are summed as:

$$\sum_{\substack{h_1, h_2=1 \\ h_1 \neq h_2}}^{N_{\text{trial}}} C_{h_1, h_2} = \sum_{\substack{h_1, h_2=1 \\ h_1 \neq h_2}}^{N_{\text{trial}}} \sum_{j_1, j_2=1}^{N_C} w_{j_1} w_{j_2} \text{Cov}\left(x_{j_1}^{(h_1)}(t), x_{j_2}^{(h_2)}(t)\right) \\ = W^T S W \quad (5)$$

Here, the matrix $S = (S_{j_1 j_2})_{1 \leq j_1, j_2 \leq N_C}$ is defined as:

$$S_{j_1 j_2} = \sum_{\substack{h_1, h_2=1 \\ h_1 \neq h_2}}^{N_{\text{trial}}} \text{Cov}\left(x_{j_1}^{(h_1)}(t), x_{j_2}^{(h_2)}(t)\right) \quad (6)$$

where, $\text{Cov}(a, b)$ refers to the covariance between a and b, N_{trial} refers to the number of training trials, h_1 and h_2 refer to the index of training trials. The periods of $x_{j_1}^{(h)}(t)$ are fixed as $t \in [t_h, t_h + T]$. Here t_h is the beginning of the h -th trial and T is the duration of the h -th trial. In order to obtain the final result, the following restriction is defined as:

$$\text{Var}(y(t)) = \sum_{j_1, j_2=1}^{N_C} w_{j_1} w_{j_2} \text{Cov}(x_{j_1}(t), x_{j_2}(t)) \\ = W^T Q W = 1 \quad (7)$$

At this point, looking for the best projection direction can be transformed into the following optimization problems:

$$\hat{w} = \arg \max_W (W^T S W) / (W^T Q W) \quad (8)$$

For the optimization, Lagrange multiplier method is effective. The optimal spatial filter is solved as the eigenvector of the matrix $Q^{-1}S$. All spatial filters corresponding to all stimulus frequencies are integrated as following equations:

$$W^m = \left[W_1^m \ W_2^m \ \dots \ W_{N_f}^m \right] \quad (9)$$

where N_f is the number of stimulus frequency. The correlation coefficient between the projection of test data $X^{(m)}$ and averaged individual template $\bar{\chi}^{(m)}$ is calculated as:

$$R_n^m = \rho((X^m)^T W^m, (\bar{\chi}_n^m)^T W^m) \quad (10)$$

Finally, correlation coefficients in different sub-bands are weighted by equation (3). The target can be identified by equation (4).

H. Performance Evaluation

To evaluate the performance of the high-speed BCIs, this study uses classification accuracy and ITR as evaluation indicators, which have been widely adopted in BCI research. The ITR can be calculated as [1]:

$$ITR = \{\log_2 N + P \log_2 P + (1 - P) \\ \times \log_2((1 - P)/(N - 1))\} \times (60/T) \quad (11)$$

where N is the number of instruction sets, P is the classification accuracy and T is consuming time for each selection, i.e., cue time plus flashing time. In this study, the consuming

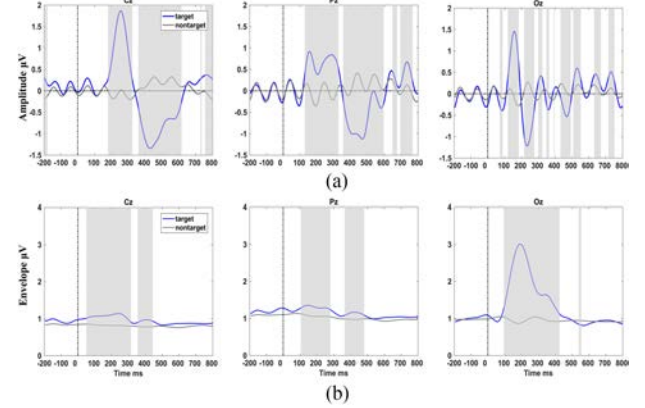


Fig. 4. (a) Transient ERPs at electrode Cz, Pz and Oz were averaged across all subjects and all sub-spellers. A band-pass filter of [1 Hz, 10 Hz] was applied to remove the SSVEP influence. (b) Grand average amplitudes of fundamental SSVEP components at electrode Cz, Pz, and Oz were displayed across all subjects and all sub-spellers. A band-pass filter between 11 and 17 Hz was applied to remove the transient ERP influence. The SSVEP amplitude was indicated by its envelope calculated by the Hilbert transform. The gray blocks presented significant statistical differences ($p < 0.05$) across subjects by paired t-tests between the target and the non-target conditions in the corresponding periods.

time was 1.7 s, 2.7 s, 3.7 s, 4.7 s, and 5.7 s for 1 to 5 rounds, respectively.

III. RESULTS

A. EEG Features Analyses

As mentioned in Introduction, the concurrent P300 and SSVEP features should have four different kinds of EEG features, i.e., time-modulated P300, frequency-phase- flickering-modulated P300, time-modulated SSVEP, and frequency-phase-modulated SSVEP. As the transient ERP is mainly distributed in the low-frequency band of 1–10 Hz while the fundamental SSVEP frequencies used in this study were higher than 12 Hz, they could be isolated from each other using different band-pass filters.

First, we analyzed the time-modulated EEG features between the target and non-target stimuli within the same sub-speller. Fig. 4(a) shows the transient ERP waveforms at Cz, Pz, and Oz, which were band-pass-filtered between 1 and 10 Hz. Consistent with previous studies, the target stimulus could induce a larger potential than the non-target stimulus. Moreover, the SSVEP feature was also discriminative between the target and non-target conditions in this study, as shown in Fig. 4(b). Specifically, the amplitude of the SSVEP recorded at Oz increased from 60 to 560 ms after the stimulus onset for the target condition but not for the non-target condition. It implies both EEG features can be used to recognize the target character within sub-speller in this study.

Then, we analyzed the frequency-phase modulated EEG features across different sub-spellers. As expected, the SSVEP waveforms induced by the short-duration SSVEP had different shapes among sub-spellers, as shown in Fig. 5. Specifically, the latency of the largest peak was the shortest for sub-speller 3 but the longest for sub-speller 10. Furthermore, sub-speller 10 had

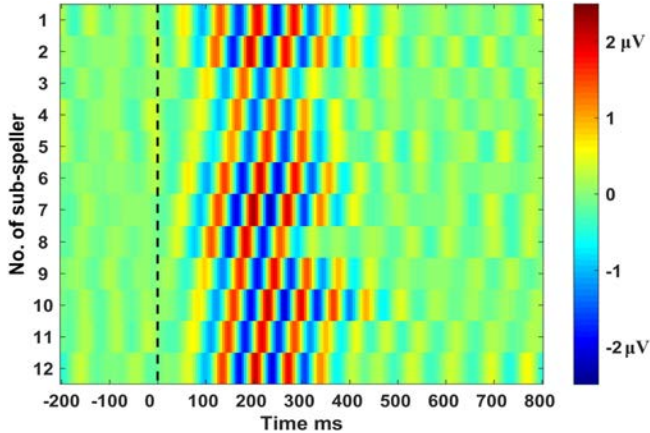


Fig. 5. The average SSVEP at electrode Oz across all subjects from -200 ms to 800 ms for each sub-speller. Time 0 represents the onset of stimulus. The band-pass filter was set to [11 Hz, 17 Hz].

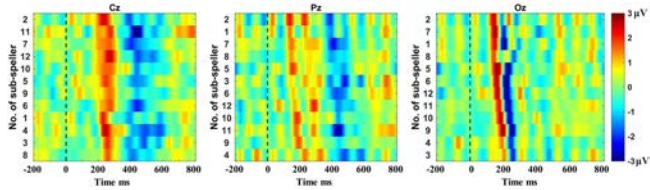


Fig. 6. ERP variations of different sub-spellers are displayed at Cz (left), Pz (middle), and Oz (right). The band-pass filter was set to [1 Hz, 10 Hz]. The temporal waveforms were averaged across all subjects for each sub-speller.

six evident SSVEP cycles while sub-speller 3 had only three evident cycles. As to the transient ERP (Fig. 6), the sub-spellers had a variety of P300 potentials recorded at both Cz and Pz. Furthermore, the P1-N1 complex recorded at Oz was also different among sub-spellers. Specifically, sub-speller 5 had the largest P1 while sub-speller 3 had the smallest one. Sub-speller 6 had the largest N1 while sub-speller 8 had the smallest one. Sub-speller 12 had the largest P300 while sub-speller 8 had the smallest one. The variability of transient ERP might be caused by the non-linear phase resetting of neural oscillations, which is sensitive to the initial conditions of background EEG [30], [32], [33].

B. Offline BCI Performance

In this section, offline accuracies were calculated and compared between single EEG features and hybrid EEG features using different classification methods. A leave-one-out cross-validation, which meant the data of 1 character was used as the test set and the data of the other 107 characters were used as the training set in each of the 108 validation steps, was adopted to ensure the robustness of the classification accuracy. Fig. 7 shows the accuracy of the sub-speller recognition against the number of rounds. It's obvious that the hybrid EEG features achieved higher accuracies than the single SSVEP feature regardless of classification methods. Specifically, compared to the single SSVEP feature, the hybrid EEG features had an improvement of 7.87%, 4.63%, 2.77%, 2.50% and 1.48% on average at 1 to 5

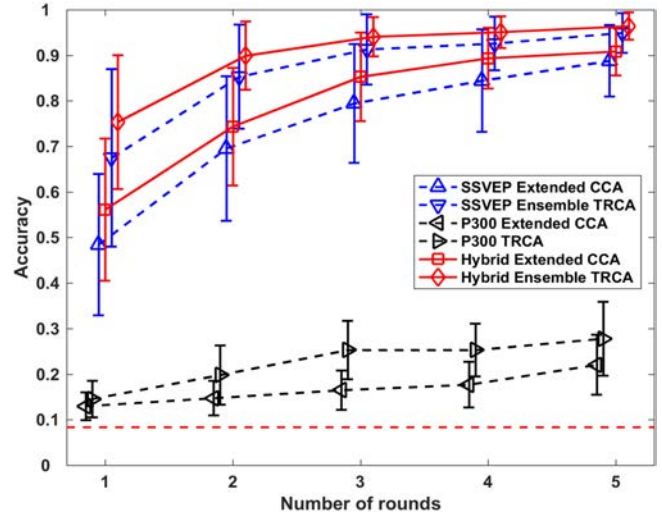


Fig. 7. Average accuracies of sub-speller recognition across subjects are displayed against the number of rounds, which are achieved by using different classification algorithms and different EEG features. The red dash line indicates the theoretical chance level of the classification (i.e., 1/12). The error bars indicated standard errors.

rounds, respectively, when using the ensemble TRCA, and had an improvement of 7.68%, 4.81%, 5.84%, 4.91% and 2.03% on average when using the extended CCA. Two-way repeated measures ANOVA showed the improvement was significant for both algorithms (ensemble TRCA: $F(1,9) = 7.95$, $p < 0.05$; extended CCA: $F(1, 9) = 8.77$, $p < 0.05$). Furthermore, the ensemble TRCA performed significantly better than extended CCA for both the single SSVEP feature ($F(1, 9) = 54.63$, $p < 0.001$) and the hybrid EEG features ($F(1, 9) = 43.24$, $p < 0.001$). Therefore, the hybrid EEG features with ensemble TRCA had the highest accuracy among all conditions, which achieved 75.37%, 89.91%, 94.07%, 95.09% and 96.39% on average at 1 to 5 rounds, respectively.

Fig. 8 shows the accuracy of the character recognition within sub-speller across rounds. For the SWLDA algorithm, the single P300 feature achieved higher accuracies than the hybrid EEG features. However, the situation reversed when using the ensemble TRCA or extended CCA as the classification method. Specifically, for the ensemble TRCA, the hybrid EEG features achieved 91.85%, 97.31%, 99.17%, 99.44% and 99.53% at 1 to 5 rounds, respectively, which were significantly higher than the single P300 feature ($F(1, 9) = 46.17$, $p < 0.001$). For the extended CCA, the hybrid EEG features brought about 82.59%, 92.96%, 97.50%, 98.89% and 98.79% at 1 to 5 rounds, respectively, which were significantly higher than the single P300 feature ($F(1, 9) = 114.82$, $p < 0.001$). Overall, the hybrid EEG features with the ensemble TRCA achieved the highest accuracy, which was significantly superior to the other conditions at first round by paired t-test (hybrid ensemble TRCA vs. hybrid extended CCA: $t_9 = 1.95 \times 10^{-3}$, $p < 0.005$; hybrid ensemble TRCA vs. hybrid SWLDA: $t_9 = 4.89 \times 10^{-7}$, $p < 0.001$; hybrid ensemble TRCA vs. P300 ensemble TRCA: $t_9 = 2.23 \times 10^{-6}$, $p < 0.001$; hybrid ensemble TRCA vs. P300 extended CCA: $t_9 = 6.49 \times 10^{-8}$, $p < 0.001$; hybrid ensemble TRCA vs. P300 SWLDA: $t_9 = 1.36 \times 10^{-5}$, $p < 0.001$; hybrid ensemble TRCA

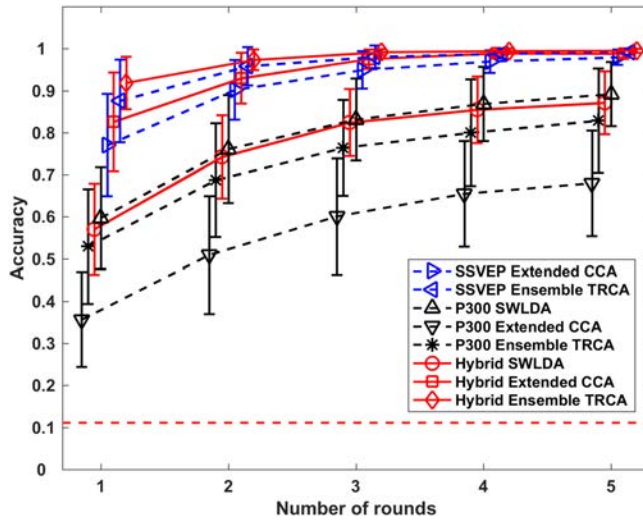


Fig. 8. Average accuracies of character recognition within sub-spellers across subjects are displayed against the number of rounds, which are achieved by using different classification algorithms and different EEG features. The red dash line indicates the theoretical chance level of the classification (i.e., 1/9). The error bars indicated standard errors.

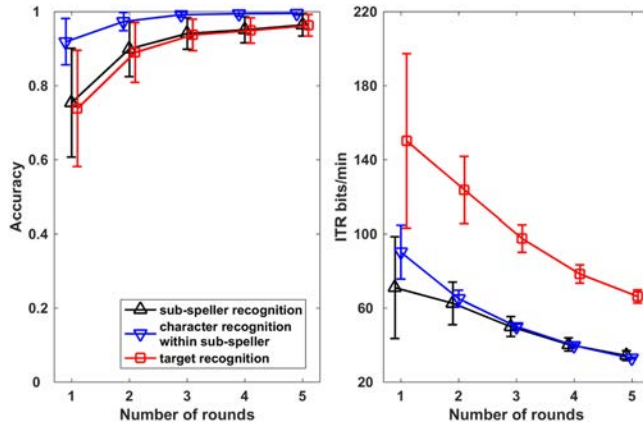


Fig. 9. The highest accuracies and the corresponding ITRs of sub-speller recognition, character recognition within sub-spellers, and overall target recognition across subjects are displayed against the number of rounds, which are achieved by using the ensemble TRCA and hybrid EEG features. The error bars indicated standard errors.

vs. SSVEP ensemble TRCA: $t_9 = 1.91 \times 10^{-2}$, $p < 0.05$; hybrid ensemble TRCA vs. SSVEP extended CCA: $t_9 = 1.65 \times 10^{-4}$, $p < 0.001$).

Fig. 9 compares the highest accuracies and the corresponding ITRs of sub-speller recognition, character recognition within sub-speller, and overall target recognition. As the combination of hybrid EEG features and ensemble TRCA performed best on recognizing both sub-spellers and characters within sub-speller, it was used to calculate the overall accuracy of target character recognition among all 108 characters. As shown in Fig. 9, the average accuracy had a rising trend against the number of rounds, which increased from 73.80% at 1 round to 96.29% at 5 rounds. The corresponding simulated online ITRs were calculated, which added another 0.7 s as the cue time for each selection. The results showed the average ITR reached a maximum of 150.09 bits/min at 1 round. Therefore, only one round was used for the following online test.

TABLE I
RESULTS OF ONLINE CUED-GUIDED SPELLING EXPERIMENTS

Subject	Consuming time (s)	Selections (Correct/Total)	Accuracy (%)	ITR (bits/min)
S1	1.7 (0.7+1)	24/24	100	238.41
S2	1.7 (0.7+1)	21/24	87.50	189.48
S3	1.7 (0.7+1)	18/24	75.00	150.29
S4	1.7 (0.7+1)	22/24	91.67	203.99
S5	1.7 (0.7+1)	17/24	70.83	138.26
S6	1.7 (0.7+1)	20/24	83.33	175.81
S7	1.7 (0.7+1)	17/24	70.83	138.26
S8	1.7 (0.7+1)	18/24	75.00	150.29
S9	1.7 (0.7+1)	21/24	87.50	189.48
S10	1.7 (0.7+1)	18/24	75.00	150.29
Max	----	----	100	238.41
Min	----	----	70.83	138.26
Mean \pm STD	----	----	81.67 \pm 9.86	172.46 \pm 32.91

TABLE II
RESULTS OF ONLINE COPY-SPELLING EXPERIMENTS

Subject	Consuming time (s)	Selections (Correct/Total)	Accuracy (%)	ITR (bits/min)
S1	1.7 (0.7+1)	17/24	70.83	138.27
S2	1.7 (0.7+1)	21/24	87.50	189.48
S3	1.7 (0.7+1)	24/24	100	238.41
S4	1.7 (0.7+1)	17/24	70.83	138.27
S5	1.7 (0.7+1)	20/24	83.33	175.81
S6	1.7 (0.7+1)	17/24	70.83	138.27
S7	1.7 (0.7+1)	18/24	75.00	150.29
S8	1.7 (0.7+1)	21/24	87.50	189.48
S9	1.7 (0.7+1)	18/24	75.00	150.29
S10	1.7 (0.7+1)	17/24	70.83	138.27
Max	----	----	100	238.41
Min	----	----	70.83	138.27
Mean \pm STD	----	----	79.17 \pm 10.02	164.69 \pm 33.32

C. Online BCI Performance

In both online cued-guided spelling and copy-spelling experiments, the classification algorithm for each subject was trained with offline data collected before the online experiment. All subjects were asked to spell 24 characters equally from 12 sub-spellers. For each selection in two online experiments, only 1.7 seconds were used, including 1 second for flickering and 0.7 second for shifting attention. The parameters of online experiments (i.e., the corresponding processing flow of output 6 and output 14 in Fig. 3) were selected according to the optimization of offline analyses (Fig. 7, Fig. 8 and Fig. 9), i.e., the time window was 50–450 ms and the ensemble TRCA algorithm was used. Specially, the sample rate was 250 Hz. The EEG signals of eight channels (Fz, Cz, Pz, PO7, PO8, O1, O2, and Oz), which were filtered by a filter bank (including eight Chebyshev Type I filters) into [X Hz, 92 Hz] ($X = 1, 11, 22, 34, 46, 58, 70$ and 82), were used for target identification.

Table I lists the results of the online cued-guided spelling tests for the ten subjects. As a result, subject 1 achieved the highest ITR of 238.41 bits/min with an accuracy of 100%. Two subjects achieved higher than 90% in accuracy and higher than 200 bits/min in ITR. The average accuracy was 81.67% and the average ITR was 172.46 bits/min across all subjects. Table II lists the results of the online copy-spelling tests. In this session, the subjects were trained to remember the position of each character

according to character distribution rule and were able to shift their fixation points very fast in 0.7 seconds. The mean accuracy was 79.17% and the mean ITR was 164.69 bits/min across the ten subjects. These results indicated the feasibility and effectiveness of the proposed high-speed BCI system with a large instruction set.

IV. DISCUSSION

A. Advantages of the Concurrent P300 and SSVEP Features

It has been demonstrated in previous studies that hybrid P300 and SSVEP features are effective in controlling BCIs. As they represent two different aspects of EEG features, i.e., from the time and frequency domains, respectively, the two features were often addressed in an independent manner to indicate the user's intent [18], [30], [42]. However, they were not two absolutely independent components when concurrently induced in this study. The frequency and phase characteristics of SSVEP can impose a great influence on the concurrent ERP, while the SSVEP duration is restricted by the target stimulus period. Therefore, besides the traditional time-modulated P300 and frequency-phase-modulated SSVEP features, two additional new EEG features, i.e., frequency-phase-flickering-modulated P300 and time-modulated SSVEP, could be elicited for the concurrent P300 and SSVEP features. As a result, the concurrent P300 and SSVEP features provide more useful information than the traditional hybrid P300 and SSVEP features for BCIs.

Although previous studies have indicated that ERPs vary with different SSVEP background, the corresponding features were too weak to be extracted and used in the past [30], [32], [33]. To deal with this problem, this study addressed the ERP variation and SSVEP as a whole rather than separate features. When taking the ERP variation as an aspect of SSVEP signals, the recognition of ERP variation could be regarded as the recognition of SSVEP differences. Because minor differences among SSVEP signals could be accurately identified using the ensemble TRCA [34], the ERP variation embedded in the SSVEP would be more effectively recognized. As expected, the results showed that adding the ERP variation into the SSVEP features led to a significant improvement in recognizing sub-spellers than purely using the SSVEP features.

Recent studies have strikingly boosted the ITR of the SSVEP-based BCIs [21], [24], [34]. However, the problem of visual fatigue still remains to be addressed for SSVEP-based BCIs. Besides our previous attempt to reduce the stimulus size [20], another remedy to this problem is to reduce the duration of SSVS. Currently, a period of 300 ms of SSVS was considered the lower limit for SSVEP classification, and a further reduction would degrade the BCI performance [34]. This study used only 200 ms of SSVS. To compensate the SSVEP degradation, a concurrent P300 feature was added to the SSVEP classification. The results demonstrated the feasibility of further shortening the SSVS duration by using the concurrent P300 and SSVEP features.

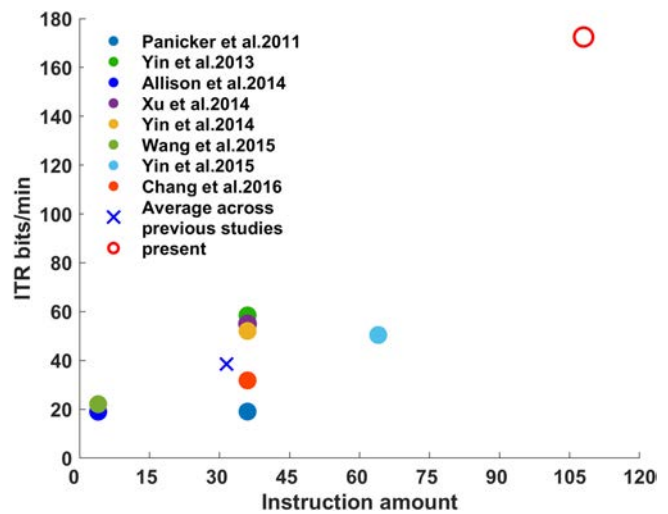


Fig. 10. A comparison of the instruction number and ITRs of online hybrid P300-SSVEP BCI spellers in the past decade (2008–2018).

B. Compare With Previous Hybrid P300-SSVEP BCI Studies

The counteraction between the instruction amount and ITR has restricted the performance of hybrid P300-SSVEP BCIs in the past. This study proposed a new P300-SSVEP BCI speller that expands the instruction set while keeping a high ITR. We further compared this study with the previous hybrid P300-SSVEP BCI studies in the last decade with a focus on online BCIs [16], [18], [19], [30], [42]–[45]. It is worth noting that since not all studies adopted copy-spelling experiment, we used the results of online cued-guided spelling experiment for comparison. The instruction number and ITR for each study are indicated by a solid dot in Fig. 10. For the previous studies, the largest instruction set contained 64 commands and the highest average ITR was 56.44 bits/min, which were much lower than those in this study. The X marks the average instruction set and ITR across previous studies, which was 31.50 commands at 38.33 bits/min. Overall, the proposed P300-SSVEP speller had almost triple numbers of instructions and quadruple ITRs relative to the traditional hybrid P300-SSVEP speller.

V. CONCLUSION

This study implements an ever-largest instruction set (over 100 command codes) for a high-speed BCI system using concurrent P300 and SSVEP features. An elaborate hybrid paradigm was developed to make a compromise between the instruction number, accuracy, and target-selection time. The ensemble TRCA algorithm was adopted to classify the concurrent P300 and SSVEP features. Consequently, only 1.7 seconds were needed for a correct target selection in online tests, resulting in a maximum ITR of 238.41 bits/min with an average of 172.46 ± 32.91 bits/min in the cue-guided spelling task and an average of 164.69 ± 33.32 bits/min in the copy-spelling task. The results demonstrate that the proposed BCI system realizes high-speed and accurate target selection from a large number of instructions, which has broad application prospects.

REFERENCES

- [1] J. R. Wolpaw *et al.*, "Brain-computer interface technology: A review of the first international meeting," *IEEE Trans. Rehabil. Eng.*, vol. 8, no. 2, pp. 164–173, Jun. 2000.
- [2] J. R. Wolpaw *et al.*, "Brain-computer interfaces for communication and control," *Clin. Neurophysiol.*, vol. 113, no. 6, pp. 767–791, 2002.
- [3] N. Liang *et al.*, "Classification of mental tasks from EEG signals using extreme learning machine," *Int. J. Neural Syst.*, vol. 16, no. 01, pp. 29–38, 2006.
- [4] C. Park *et al.*, "Classification of motor imagery BCI using multivariate empirical mode decomposition," *IEEE Trans. Neural Syst. Rehabil. Eng.*, vol. 21, no. 1, pp. 10–22, Jan. 2013.
- [5] S. Gao *et al.*, "Visual and auditory brain-computer interfaces," *IEEE Trans. Biomed. Eng.*, vol. 61, no. 5, pp. 1436–1447, May 2014.
- [6] J. Feng *et al.*, "Towards correlation-based time window selection method for motor imagery BCIs," *Neural Netw.*, vol. 102, pp. 87–95, 2018.
- [7] K. Wang *et al.*, "Enhance decoding of pre-movement EEG patterns for brain-computer interfaces," *J. Neural Eng.*, vol. 17, no. 1, 2020, Art. no. 016033.
- [8] Q. Gao *et al.*, "Noninvasive electroencephalogram based control of a robotic arm for writing task using hybrid BCI system," *Biomed. Res. Int.*, vol. 2017, 2017, Art. no. 8316485.
- [9] M. Salvaris and F. Sepulveda, "Visual modifications on the P300 speller BCI paradigm," *J. Neural Eng.*, vol. 6, no. 4, 2009, Art. no. 046011.
- [10] G. Townsend and V. Platsko, "Pushing the P300-based brain-computer interface beyond 100 bpm: Extending performance guided constraints into the temporal domain," *J. Neural Eng.*, vol. 13, no. 2, 2016, Art. no. 026024.
- [11] X. Xiao *et al.*, "Discriminative canonical pattern matching for single-trial classification of ERP components," *IEEE Trans. Biomed. Eng.*, vol. 67, no. 8, pp. 2266–2275, Aug. 2020.
- [12] D. Ryan *et al.*, "Evaluating brain-computer interface performance using color in the P300 checkerboard speller," *Clin. Neurophysiol.*, vol. 128, no. 10, pp. 2050–2057, 2017.
- [13] Y. Wang *et al.*, "A practical VEP-based brain-computer interface," *IEEE Trans. Neural Syst. Rehabil. Eng.*, vol. 14, no. 2, pp. 234–240, Jun. 2006.
- [14] Y. Wang *et al.*, "Brain-computer interfaces based on visual evoked potentials," *IEEE Eng. Med. Biol. Mag.*, vol. 27, no. 5, pp. 64–71, Sep.–Oct. 2008.
- [15] X. Chen *et al.*, "A high-itr ssvep-based bci speller," *Brain-Comput. Interfaces*, vol. 1, no. 3-4, pp. 181–191, 2014.
- [16] R. C. Panicker *et al.*, "An asynchronous P300 BCI with SSVEP-based control state detection," *IEEE Trans. Biomed. Eng.*, vol. 58, no. 6, pp. 1781–1788, Jun. 2011.
- [17] M. Xu *et al.*, "A hybrid BCI speller paradigm combining P300 potential and the SSVEP blocking feature," *J. Neural Eng.*, vol. 10, no. 2, 2013, Art. no. 026001.
- [18] E. Yin *et al.*, "A novel hybrid BCI speller based on the incorporation of SSVEP into the P300 paradigm," *J. Neural Eng.*, vol. 10, no. 2, 2013, Art. no. 026012.
- [19] E. Yin *et al.*, "A speedy hybrid BCI spelling approach combining P300 and SSVEP," *IEEE Trans. Biomed. Eng.*, vol. 61, no. 2, pp. 473–483, Feb. 2014.
- [20] M. Xu *et al.*, "A brain-computer interface based on miniature- event-related potentials induced by very small lateral visual stimuli," *IEEE Trans. Biomed. Eng.*, vol. 65, no. 5, pp. 1166–1175, May 2018.
- [21] X. Chen *et al.*, "High-speed spelling with a noninvasive brain-computer interface," *Proc. Nat. Acad. Sci.*, vol. 112, no. 44, pp. E6058–E6067, 2015.
- [22] L. A. Farwell and E. Donchin, "Talking off the top of your head: Toward a mental prosthesis utilizing event-related brain potentials," *Electroencephalogr. Clin. Neurophysiol.*, vol. 70, no. 6, pp. 510–523, 1988.
- [23] H. Hwang *et al.*, "Development of an SSVEP-based BCI spelling system adopting a QWERTY-style LED keyboard," *J. Neurosci. Methods*, vol. 208, no. 1, pp. 59–65, 2012.
- [24] X. Chen *et al.*, "Filter bank canonical correlation analysis for implementing a high-speed SSVEP-based brain-computer interface," *J. Neural Eng.*, vol. 12, no. 4, 2015, Art. no. 046008.
- [25] G. Townsend *et al.*, "A novel P300-based brain-computer interface stimulus presentation paradigm: Moving beyond rows and columns," *Clin. Neurophysiol.*, vol. 121, no. 7, pp. 1109–1120, 2010.
- [26] J. Jin *et al.*, "An adaptive P300-based control system," *J. Neural Eng.*, vol. 8, no. 3, 2011, Art. no. 036006.
- [27] J. Jin *et al.*, "Targeting an efficient target-to-target interval for P300 speller brain-computer interfaces," *Med. Biol. Eng. Comput.*, vol. 50, no. 3, pp. 289–296, 2012.
- [28] M. Nakanishi *et al.*, "Generating visual flickers for eliciting robust steady-state visual evoked potentials at flexible frequencies using monitor refresh rate," *PLoS One*, vol. 9, no. 6, 2014, Art. no. e99235.
- [29] M. Nakanishi *et al.*, "A high-speed brain speller using steady-state visual evoked potentials," *Int. J. Neural Syst.*, vol. 24, no. 06, 2014, Art. no. 1450019.
- [30] M. Xu *et al.*, "A visual parallel-BCI speller based on the time-frequency coding strategy," *J. Neural Eng.*, vol. 11, no. 2, 2014, Art. no. 026014.
- [31] X. Fan *et al.*, "A brain-computer interface-based vehicle destination selection system using P300 and SSVEP signals," *IEEE Trans. Intell. Transp. Syst.*, vol. 16, no. 1, pp. 274–283, Feb. 2015.
- [32] M. Xu *et al.*, "Use of a steady-state baseline to address evoked vs. oscillation models of visual evoked potential origin," *Neuroimage*, vol. 134, pp. 204–212, 2016.
- [33] M. Xu *et al.*, "Fast detection of covert visuospatial attention using hybrid N2pc and SSVEP features," *J. Neural Eng.*, vol. 13, no. 6, 2016, Art. no. 066003.
- [34] M. Nakanishi *et al.*, "Enhancing detection of SSVEPs for a high-speed brain speller using task-related component analysis," *IEEE Trans. Biomed. Eng.*, vol. 65, no. 1, pp. 104–112, Jan. 2018.
- [35] Y. Wang *et al.*, "A benchmark dataset for SSVEP-based brain-computer interfaces," *IEEE Trans. Neural Syst. Rehabil. Eng.*, vol. 25, no. 10, pp. 1746–1752, Oct. 2017.
- [36] Z. Yao *et al.*, "An online brain-computer interface in mobile virtual reality environments," *Integr. Comput.-Aided Eng.*, vol. 26, no. 4, pp. 345–360, 2019.
- [37] D. J. Krusienski *et al.*, "A comparison of classification techniques for the P300 Speller," *J. Neural Eng.*, vol. 3, no. 4, 2006, Art. no. 299.
- [38] Z. Lin *et al.*, "Frequency recognition based on canonical correlation analysis for SSVEP-based BCIs," *IEEE Trans. Biomed. Eng.*, vol. 53, no. 12, pp. 2610–2614, Dec. 2006.
- [39] G. Bin *et al.*, "An online multi-channel SSVEP-based brain-computer interface using a canonical correlation analysis method," *J. Neural Eng.*, vol. 6, no. 4, 2009, Art. no. 046002.
- [40] X. Xing *et al.*, "A high-speed SSVEP-based BCI using dry EEG electrodes," *Sci. Rep.*, vol. 8, no. 1, 2018, Art. no. 14708.
- [41] H. Tanaka *et al.*, "Task-related component analysis for functional neuroimaging and application to near-infrared spectroscopy data," *Neuroimage*, vol. 64, pp. 308–327, 2013.
- [42] E. Yin *et al.*, "A hybrid brain-computer interface based on the fusion of P300 and SSVEP scores," *IEEE Trans. Neural Syst. Rehabil. Eng.*, vol. 23, no. 4, pp. 693–701, Jul. 2015.
- [43] B. Z. Allison *et al.*, "A four-choice hybrid P300/SSVEP BCI for improved accuracy," *Brain-Comput. Interfaces*, vol. 1, no. 1, pp. 17–26, 2014.
- [44] M. Wang *et al.*, "A new hybrid BCI paradigm based on P300 and SSVEP," *J. Neurosci. Methods*, vol. 244, pp. 16–25, 2015.
- [45] M. H. Chang *et al.*, "Eliciting dual-frequency SSVEP using a hybrid SSVEP-P300 BCI," *J. Neurosci. Methods*, vol. 258, pp. 104–113, 2016.